Chemistry–A European Journal

Research Article
doi.org/10.1002/chem.202501787

Chemistry Europe
European Chemical Societies Publishing

www.chemeurj.org

Accessing Single-Molecule Properties of Heptacene Using a Metal-Organic Framework

Takumi Miura,[a] Takashi Kitao,[b] Keigo E. Yamada,[a] Yee Seng Chan,[c] Hironobu Hayashi,[d] Hiroko Yamada,[e] and Takashi Uemura*[a]

Acenes, classic polycyclic aromatic hydrocarbons composed of linearly fused benzene rings, represent a model system for exploring the physical properties of 1D π-conjugated structures. Isolating individual molecules at the single-molecule level provides a means to investigate their intrinsic properties, which is typically done by dissolving in solutions. However, this approach becomes increasingly difficult to apply for higher acenes owing to their high insolubility and instability. Thus, the electronic structure of higher acenes has long been a subject of intense discussion. This paper introduces a method to encapsulate heptacene within a metal-organic framework (MOF) through in situ photochemical conversion of a precursor molecule. The transformation reaction of the precursor is significantly accelerated upon inclusion. This approach stabilizes otherwise unstable heptacene by suppressing undesirable side reactions through the spatial constraint. The bulk production of heptacene in an isolated state enables its exploration through various analytical techniques, providing insights into its single-molecule properties and leading to the first observation of its fluorescence. Moreover, experimental and theoretical studies reveal the electronic ground state of pristine heptacene.

Acenes, consisting of linearly annulated benzene rings, have attracted significant research attention owing to their diverse physical properties.[1–5] As the number of benzene rings increases, acenes exhibit exceptional optical, electronic, and magnetic functions, rendering them promising for use in various technological domains.[6,7] Investigating the properties of single acene molecules is key to understanding the mechanisms underlying the functionalities of acenes.[8] Conventionally, single-molecule properties are studied in solution. However, research on acenes longer than hexacene, referred to as higher acenes, has been hindered by their poor solubility and instability.[9–13] Although the introduction of solubilizing and stabilizing substituents can address this problem, such modifications compromise the inherent properties of the molecules.[14] On-surface synthesis has recently emerged as a promising alternative for producing single-molecule higher acenes without any substituents, providing valuable insights into the properties of individual molecules.[15,16] However, the strong electronic coupling between the acenes and underlying metal substrates may affect their physical properties.[10,17–19] Moreover, higher acenes can only exist under ultra-high vacuum conditions on the surface because of their chemical instability, as explained by Clar's aromatic π-sextet rule. Furthermore, the limited reaction areas result in an exceedingly small yield of products, restricting the application of various characterization techniques.

To address these challenges, this study introduces a novel strategy based on host–guest chemistry to investigate the single-molecule properties of unstable higher acenes. Metal-organic frameworks (MOFs), which are nanoporous materials composed of metal ions and organic ligands, have gained increasing attention for potential application in numerous fields, such as gas storage, separation, catalysis, and drug delivery.[20–24] In particular, the tunable nanospaces of MOFs offer an ideal compartment for controlling the assemblies of guest species.[25–28] Additionally, their crystalline arrangement ensures that the nanochannels are uniform across the entire material. Therefore, confining molecules within MOF nanochannels can help create a single-molecule-like state akin to that in solution while maintaining a bulk solid phase, thus expanding the scope of possible analytical methods.

As a proof of concept, we attempted to encapsulate heptacene into the nanochannels. However, heptacene is

[a] Dr. T. Miura, Dr. K. E. Yamada, Prof. T. Uemura
Department of Applied Chemistry, Graduate School of Engineering, The University of Tokyo, 7–3–1 Hongo, Bunkyo-ku, Tokyo 113–8656, Japan
E-mail: uemurat@g.ecc.u-tokyo.ac.jp

[b] Dr. T. Kitao
Nanocarbon Material Research Institute, National Institute of Advanced Industrial Science and Technology (AIST), Tsukuba Central 5, 1-1-1 Higashi, Tsukuba, Ibaraki 305–8565, Japan

[c] Dr. Y. S. Chan
Division of Materials Science, Nara Institute of Science and Technology (NAIST), 8916-5 Takayama-cho, Ikoma, Nara 630-0192, Japan

[d] Dr. H. Hayashi
Center for Basic Research on Materials, National Institute for Materials Science (NIMS), 1-2-1 Sengen, Tsukuba, Ibaraki 305-0047, Japan

[e] Prof. H. Yamada
Institute for Chemical Research, Kyoto University, Gokasho, Uji, Kyoto 611-0011, Japan

Supporting information for this article is available on the WWW under https://doi.org/10.1002/chem.202501787

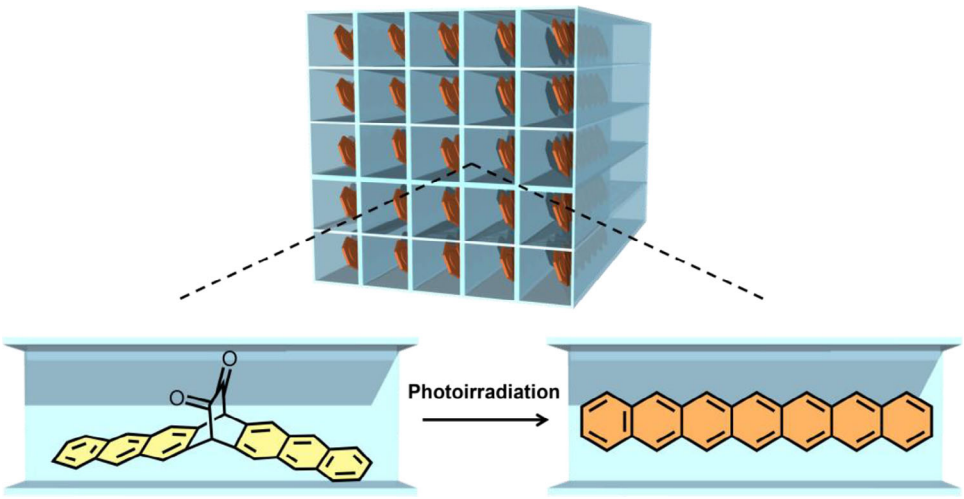

Figure 1. Schematic of in situ conversion of DEH to heptacene within an MOF.

insoluble and unstable, rendering its direct insertion into MOFs unfeasible.[29–31] Therefore, we synthesize heptacene within an MOF by introducing 7,16-dihydro-7,16-ethanoheptacene-19,20-dione (DEH), a soluble and stable precursor, into the nanochannels and then inducing its photochemical reaction (Figure 1). The reactivity of DEH molecules within the MOF nanochannels is considerably higher than in its crystalline solid state. Compared with that in solution, the lifetime of heptacene is extended through the suppression of oxidation and dimerization reactions within the nanopores, permitting extensive characterizations. The bulk production of isolated heptacene molecules enables the first experimental observation of its fluorescence, providing insights into the elusive electronic ground state of pristine heptacene. Overall, the proposed method can help fully leverage the functionalities of chemically unstable molecules and expand our understanding of the nature of higher acenes.

Initially, we synthesized bulk heptacene through the solid-state conversion of neat DEH. A photoconversion experiment was conducted under reduced pressure and at room temperature using a light-emitting diode as the light source. A wavelength of 467 nm was selected owing to its proximity to the n–π^* transition of the diketone group of DEH. A transparent KBr film containing dispersed DEH powder was prepared to ensure thorough illumination of the sample and facilitate deeper light penetration. Fourier-transform infrared (FT-IR) spectroscopy was conducted to analyze the product structure. The out-of-plane (*opla*) sp^2 C—H vibration modes were classified as SOLO, DUO, TRIO, or QUATRO, based on the number of adjacent C—H groups. As the number of terminal C—H groups remained unchanged after the transformation reaction, the conversion ratios of DEH were determined by analyzing the relative peak intensities of the α-diketone moiety (1735 cm^{-1}) and *opla* aromatic C—H vibration QUATRO mode (742 cm^{-1}).[32,33] The reaction efficiency was highly dependent on the light intensity. At an irradiation power of 50 $mWcm^{-2}$, the conversion reaction proceeded slowly with the reaction ratio of DEH being only 30% after photoirradiation for 90 minutes (Figure S1). Complete conversion of DEH in the solid state was achieved by increasing the light power from 50 to 200 $mWcm^{-2}$, as evidenced by the disappearance of the peak for the α-diketone moiety of DEH in the FT-IR spectra (Figure S1). However, along with the characteristic peaks for heptacene, an additional peak was detected at 2950 cm^{-1}. Based on the simulated spectra (Figure S2), this peak was attributed to the sp^3 C—H vibration mode of diheptacene, indicating that part of the heptacene dimerized to form diheptacene owing to its inherent diradical character.[34] For the cycloreversion of diheptacene, the product was annealed at 300 °C under vacuum, yielding pure heptacene in the bulk state (Figure S1).[35]

To obtain heptacene in the single-molecule state, we used an MOF, $[Al(OH)(L)]_n$ (L = dicarboxylate), with 1D nanochannels as the host. This system afforded precise control over the pore size by varying the dicarboxylate ligand, L.[36] Additionally, this MOF did not exhibit any absorption at the irradiation wavelength. Considering the molecular size of DEH (18 × 7 × 6 $Å^3$), $[Al(OH)(bpdc)]_n$ (**1**; bpdc = 4,4-biphenyldicarboxylate; pore size = 11 × 11 $Å^2$) could accommodate single DEH molecules within its nanochannels (Figure 2a). DEH was introduced into the MOF by soaking the host crystals in a saturated acetone solution containing DEH at room temperature for 72 hours. The resulting light-yellow solid was filtered and washed with $CHCl_3$ and acetone to remove the surface-adsorbed DEH, affording the nanocomposite of **1** with DEH (**1**⊃DEH). The powder X-ray diffraction (PXRD) pattern of **1**⊃DEH, compared with that of the original host, indicated that the crystal structure was maintained upon the encapsulation of DEH (Figure 2b). The absence of diffraction peaks corresponding to DEH confirmed the lack of deposition of DEH on the crystal surface of **1**. This observation was also supported by scanning electron microscopy (SEM) and particle size distribution measurements (Figures S3, S4). Furthermore, the gas adsorption isotherm of **1**⊃DEH showed a decrease in its adsorption capacity compared with that of **1** (Figure S5). These results confirmed the full encapsulation of DEH within the MOF nanochannels. To evaluate the loading amount of DEH in **1**, DEH was extracted using $CDCl_3$ after dissolving **1** in 1 M sodium ethylenediaminetetraacetate aqueous solution. Dimethyl terephthalate was used as the internal standard. Proton nuclear

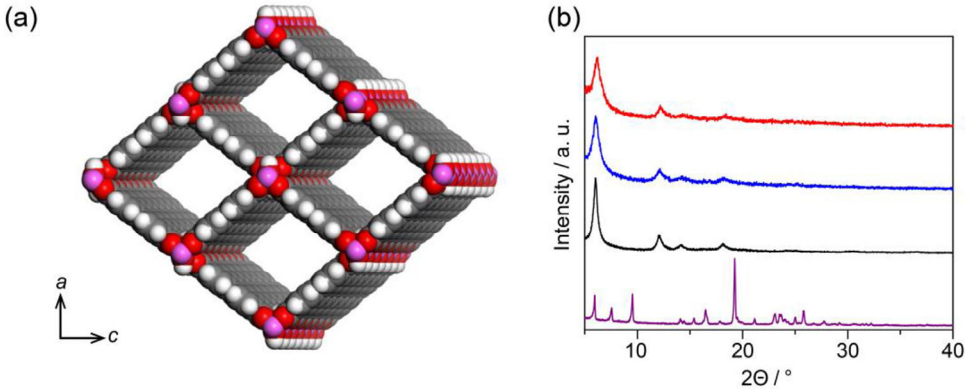

Figure 2. a) Crystal structure of **1** (Al, pink; O, red; C, gray; H, white). b) PXRD patterns of DEH (purple), **1** (black), **1**⊃DEH (blue), and **1**⊃heptacene (red).

magnetic resonance (^{1}H-NMR) analysis revealed that the number of DEH molecules per unit cell of **1** was 0.04 (Figure S6; details can be found in the supporting information).

1⊃DEH powder was placed between two glass slides and exposed to light at 50 mWcm^{-2}, resulting in the quantitative formation of the nanocomposite of **1** including heptacene (**1**⊃heptacene). During irradiation, the sample color changed from light yellow to light brown, suggesting the conversion of DEH to heptacene with an extended conjugated structure. The PXRD pattern of **1**⊃heptacene was consistent with that of the pristine host, confirming that the structure of **1** was preserved during the irradiation (Figure 2b). Furthermore, SEM images showed that the size and morphology of the MOF particles remained unchanged after irradiation (Figure S3). These results confirmed the incorporation of heptacene within the nanochannels of MOF **1**. The consumption ratio of DEH was determined through the ^{1}H-NMR analysis of DEH extracted from the MOF before and after photoirradiation. As 90 minutes of irradiation, the resonance peaks corresponding to DEH significantly diminished (Figure S6). This observation demonstrated the formation of heptacene through quantitative conversion, suggesting that the geometrical constraint of the host MOF effectively suppressed dimerization within **1**.[35] Notably, DEH within the MOF particles underwent complete conversion at a low power of 50 mWcm^{-2}, in contrast to the bulk DEH under identical conditions (only 30% conversion). In the bulk condition, the DEH powder was dispersed in a transparent KBr film, effectively minimizing light scattering and ensuring more efficient light exposure to the sample. Despite this, **1**⊃DEH showed higher conversion efficiency, likely owing to the difference in the aggregation state of DEH. The transformation reaction of DEH necessitates substantial structural changes, which are restricted owing to the dense packing of DEH molecules in the bulk crystalline state (Figure 3a).[37] In contrast, DEH molecules in the MOF were isolated in the single-molecule state, which likely facilitated the conversion reaction. Molecular dynamics (MD) simulations of **1**⊃DEH provided deeper insights into the effect of the nanoconfinement on the conversion reaction. Upon encapsulation, the dihedral angle between the two aromatic regions bridged by the diketone moiety increased from 125° to 152° via the host–guest π–π interactions, thereby lowering the reaction barrier for α-diketone cleavage (Figure 3b).[15,18,38,39]

Although the dissolution of DEH enables high-efficiency transformation reactions, the resulting heptacene in solutions inevitably undergoes immediate dimerization and/or oxidation.[37] In contrast, the bulk heptacene prepared by the solid-state conversion of DEH was found to be stable, with no undesirable side reactions observed for at least one month (Figure S1). Recent studies have demonstrated such high stability of higher acenes in the solid state,[40–42] attributable to the robust intermolecular packing that prevents oxygen access and suppresses dimerization, as suggested by the aggregation structure of heptacene (Figures S7, 8). Entrapment within MOFs can stabilize otherwise unstable higher acenes through the geometrical constraint of the nanopores. Consequently, despite being in a single-molecule state, similar to that in solution, heptacene can be handled as a solid. Thus, the proposed approach represents a promising route to access the single-molecule physical properties of heptacene using various characterization methods.

To demonstrate this advantage, we investigated the stability of heptacene within the MOF. When **1**⊃heptacene was stored in an N_2 environment under dark conditions, the absorbance of heptacene remained nearly constant over time, attributable to the suppression of dimerization (Figure S9). Moreover, heptacene remained detectable for several hours even under ambient air, owing to the restricted access of oxygen to the heptacene molecules. In contrast, heptacene in solution and polymer matrices has been noted to rapidly decompose through dimerization and/or oxidation reactions.[37,41] These findings highlight that the combination of the precursor method and host–guest chemistry provides a promising approach for stabilizing typically unstable heptacene, enabling the exploration of its single-molecule optoelectronic properties.

The ultraviolet/visible/near IR (UV/vis/NIR) spectrum of bulk heptacene exhibited the S_0 to S_1 transition band (p-band) from 600 to 850 nm (Figure 4a).[37,43] Additionally, broad bands were detected around 850–1100 nm, attributable to the charge-transfer exciton coupling between nearest-neighbor heptacene molecules.[44] The absorption spectrum of **1**⊃heptacene also showed the S_0 to S_1 transition band of heptacene. The energy gap of heptacene in **1** was calculated to be 1.46 eV from the edge of the absorption band, similar to the value (1.50 eV) reported for heptacene dispersed in the polymer matrix.[43] A

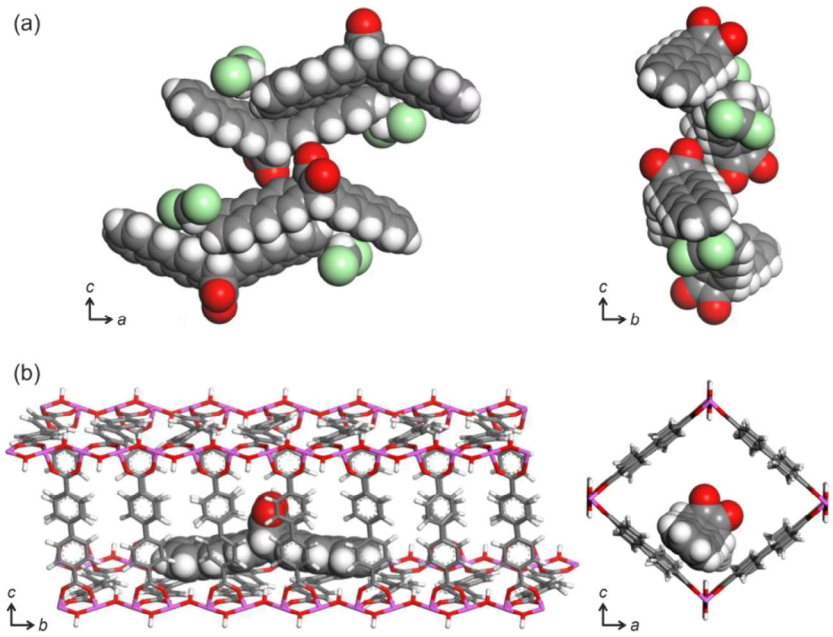

Figure 3. a) Crystal structure of DEH containing dichloromethane as the synthetic solvent.[37] b) MD structure of DEH confined within the nanochannels of **1** (Al, pink; O, red; C, gray; Cl, light green; H, white).

blue shift in the maximum absorption wavelength was observed for **1**⊃heptacene (775 nm) compared to bulk heptacene (811 nm). The peaks of p-band were sharpened compared with those of the bulk heptacene. Moreover, intermolecular exciton coupling bands were not observed. These results indicate that the absorption bands originated from electronically decoupled single heptacene molecules, as supported by the modeled structure of **1**⊃heptacene (Figure 4b).[43,45,46]

The isolation of heptacene within the MOF enabled the detection of its emission properties for the first time. In general, unsubstituted π-conjugated materials, including acenes, suffer from aggregation-induced quenching in the solid state; therefore, their emission characteristics are typically investigated by dissolving in solutions.[47] However, higher acenes without any peripheral substitutions are insoluble and chemically unstable,[48,49] and to the best of our knowledge, their emission properties have not yet been reported. When emission measurements for **1**⊃heptacene were conducted at room temperature, no emission was detected, consistent with the results for bulk heptacene. According to the energy gap rule, the emission quantum yield of acenes decreases as the number of benzene rings increases. Therefore, the emission intensity of heptacene was likely below the detection limit.[48,49] Low-temperature measurements are effective for substances with low quantum yields owing to reduced molecular motion and nonradiative deactivation. Thus, we performed emission measurements at 77 K. Emission signals were successfully detected from 860 to 1000 nm, unlike the results for bulk heptacene (Figure 4c).[31,50] The observed emission wavelength was comparable with the value predicted by time-dependent density-functional theory calculations of closed-shell heptacene, confirming that the emission was attributable to fluorescence from the S_1 to S_0 states of heptacene (Figure 4d).

According to theoretical predictions, the open-shell diradical character of acenes intensifies with increasing acene length.[51,52] To clarify the electronic structures, electron spin resonance (ESR) measurements of higher acenes with solubilizing substituents have been conducted in solutions, revealing the presence of radical species. However, the corresponding temperature dependence remains elusive owing to the thermal instability of these acenes.[53,54] Indeed, variable temperature ESR of the bulk heptacene dispersed in a KBr film has failed to clarify its electronic structure owing to the occurrence of pyrolysis before the singlet to triplet thermal transition (Figure S10). Scanning tunneling spectroscopy is a powerful method to investigate the electronic structures of single unsubstituted higher acenes.[15] However, strong electronic interactions between acene molecules and metal surfaces could induce undesirable changes in the electronic structures.[18] Therefore, elucidating the intrinsic electronic structures of higher acenes remains a formidable task. The spectroscopic analysis of single heptacene molecules within the MOF highlighted the electronic ground state of pristin heptacene. The absorption and fluorescence wavelengths of **1**⊃heptacene were similar to predictions for a closed-shell configuration (Figures 4d, S11). This result demonstrates that the ground state of heptacene with seven fused benzene rings within the MOF is predominantly closed-shell singlet.

In conclusion, we have demonstrated that the conversion of the precursor within the MOF is an effective strategy for elucidating the single-molecule properties and electronic ground state of unstable higher acenes. Precursor conversion within MOFs enables the synthesis and in-depth characterization of acenes larger than heptacene. As our technique yields bulk quantities of isolated higher acenes, we believe that this approach helps enhance our understanding of the effects of intermolecular interactions on the remarkable properties of these higher

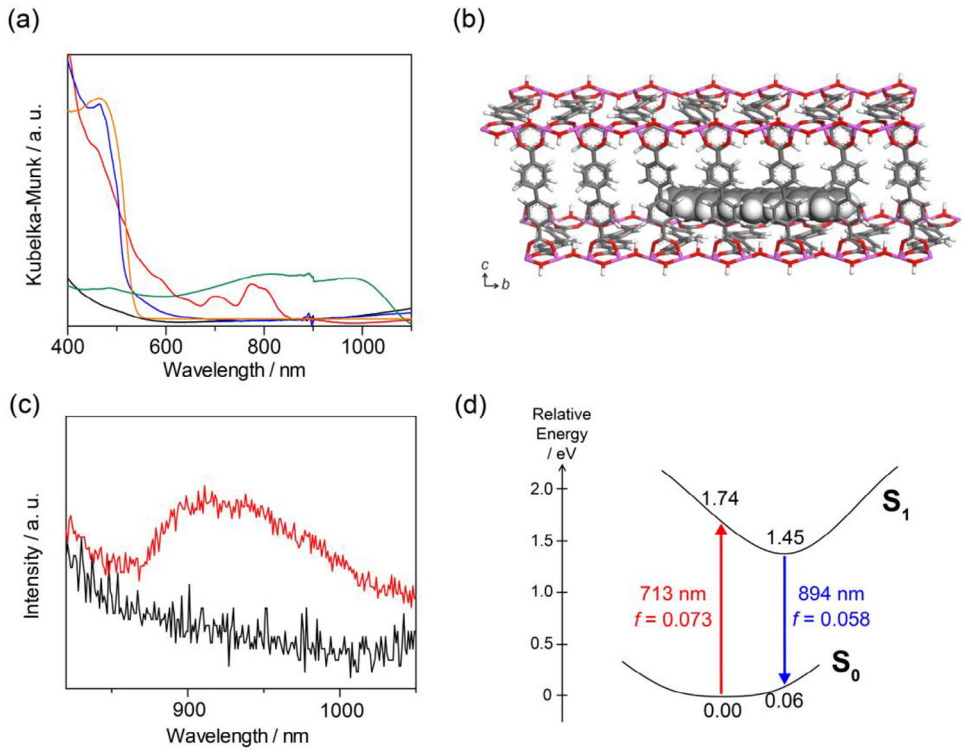

Figure 4. a) UV/vis/NIR absorption spectra of DEH (orange), bulk heptacene (green), **1** (black), **1**⊃DEH (blue), and **1**⊃heptacene (red). b) MD structure of **1**⊃heptacene, showing the nanoconfinement of single heptacene molecules within the MOF nanochannels (Al, pink; O, red; C, gray; H, white). c) Emission spectra of bulk heptacene (black) and **1**⊃heptacene (red) at 77 K (excitation wavelength of 705 nm). d) Schematic of potential energy surfaces of closed-shell heptacene, calculated at RCAM-B3LYP-D3(BJ)/6–311++G(3d2f,3p2d). f denotes the oscillator strength of transition.

acenes, such as their diradical (and even polyradical) character and singlet fission.[9,10,42,55,56] Moreover, this methodology can be extended to other unstable and insoluble compounds, paving the way for their diverse applications.

Acknowledgments

This work was supported by the JST CREST (JPMJCR20T3) and PRESTO (JPMJPR21A7) programs, Ogasawara Foundation for the Promotion of Science and Engineering, and a Grant-in-Aid for Scientific Research (JP24K01276) and the Japan Society for the Promotion of Science (JSPS) Fellows (JP23KJ0539) from the Ministry of Education, Culture, Sports, Science, and Technology, Government of Japan. The computation was performed using Research Center for Computational Science, Okazaki, Japan (Project: 24-IMS-C324). We thank K. Nakabayashi (The University of Tokyo) for assisting with fluorescence measurements.

Conflict of Interest

The authors declare no conflict of interest.

Data Availability Statement

The data that support the findings of this study are available from the corresponding author upon reasonable request.

Keywords: acenes · host — guest systems · metal-organic frameworks · microporous materials · optoelectronic properties

[1] J. E. Anthony, *Chem. Rev.* **2006**, *106*, 5028.
[2] K. Tateishi, M. Negoro, S. Nishida, A. Kagawa, Y. Morita, M. Kitagawa, *Proc. Natl. Acad. Sci. USA* **2014**, *111*, 7527.
[3] D. G. Bossanyi, M. Matthiesen, S. Wang, J. A. Smith, R. C. Kilbride, J. D. Shipp, D. Chekulaev, E. Holland, J. E. Anthony, J. Zaumseil, A. J. Musser, J. Clark, *Nat. Chem.* **2021**, *13*, 163.
[4] O. S. Lee, N. Sharma, T. Matulaitis, A. M. Z. Slawin, Y. Olivier, I. D. W. Samuel, M. C. Gather, E. Zysman-Colman, *J. Mater. Chem. C* **2024**, *12*, 4273.
[5] L. Lerena, R. Zuzak, S. Godlewski, A. M. Echavarren, *Chem. Eur. J.* **2024**, *30*, e202402122.
[6] F. Eisenhut, T. Kühne, F. García, S. Fernández, E. Guitián, D. Pérez, G. Trinquier, G. Cuniberti, C. Joachim, D. Peña, F. Moresco, *ACS Nano* **2020**, *14*, 1011.
[7] M. Müller, L. Ahrens, V. Brosius, J. Freudenberg, U. H. F. Bunz, *J. Mater. Chem. C* **2019**, *7*, 14011.
[8] S. Fujii, S. Kaneko, L. Chenyang, M. Kiguchi, *Appl. Surf. Sci.* **2015**, *354*, 362.
[9] Z. Ruan, J. Schramm, J. B. Bauer, T. Naumann, H. F. Bettinger, R. Tonner-Zech, J. M. Gottfried, *J. Am. Chem. Soc.* **2024**, *146*, 3700.
[10] R. Zuzak, M. Kumar, O. Stoica, D. Soler-Polo, J. Brabec, K. Pernal, L. Veis, R. Blieck, A. M. Echavarren, P. Jelinek, S. Godlewski, *Angew. Chem. Int. Ed.* **2024**, *63*, e202317091.
[11] B. Shen, J. Tatchen, E. Sanchez-Garcia, H. F. Bettinger, *Angew. Chem. Int. Ed.* **2018**, *57*, 10506.
[12] M. Watanabe, Y. J. Chang, S.-W. Liu, T.-H. Chao, K. Goto, M. M. Islam, C.-H. Yuan, Y.-T. Tao, T. Shinmyozu, T. J. Chow, *Nat. Chem.* **2012**, *4*, 574.
[13] H. Yamada, H. Hayashi, *Photochem. Photobiol. Sci.* **2022**, *21*, 1511.
[14] X. Shi, C. Chi, *Chem. Rec.* **2016**, *16*, 1690.

[15] J. I. Urgel, S. Mishra, H. Hayashi, J. Wilhelm, C. A. Pignedoli, M. Di Giovannantonio, R. Widmer, M. Yamashita, N. Hieda, P. Ruffieux, H. Yamada, R. Fasel, *Nat. Commun.* **2019**, *10*, 861.
[16] R. Zuzak, R. Dorel, M. Kolmer, M. Szymonski, S. Godlewski, A. M. Echavarren, *Angew. Chem. Int. Ed.* **2018**, *57*, 10500.
[17] P. Grüninger, M. Polek, M. Ivanović, D. Balle, R. Karstens, P. Nagel, M. Merz, S. Schuppler, R. Ovsyannikov, H. F. Bettinger, H. Peisert, T. Chassé, *J. Phys. Chem. C* **2018**, *122*, 19491.
[18] M. Zugermeier, M. Gruber, M. Schmid, B. P. Klein, L. Ruppenthal, P. Müller, R. Einholz, W. Hieringer, R. Berndt, H. F. Bettinger, J. M. Gottfried, *Nanoscale* **2017**, *9*, 12461.
[19] T. Boné, A. Windischbacher, L. Scheucher, F. Presel, P. Schnabl, M. S. Wagner, H. F. Bettinger, H. Peisert, T. Chassé, P. Puschnig, M. G. Ramsey, M. Sterrer, G. Koller, *J. Phys. Condens. Matter.* **2023**, *35*, 475003.
[20] S. Kitagawa, R. Kitaura, S.-i. Noro, *Angew. Chem. Int. Ed.* **2004**, *43*, 2334.
[21] H. Furukawa, K. E. Cordova, M. O'Keeffe, O. M. Yaghi, *Science* **2013**, *341*, 1230444.
[22] K. Sumida, D. L. Rogow, J. A. Mason, T. M. McDonald, E. D. Bloch, Z. R. Herm, T.-H. Bae, J. R. Long, *Chem. Rev.* **2012**, *112*, 724.
[23] J. Lee, O. K. Farha, J. Roberts, K. A. Scheidt, S. T. Nguyen, J. T. Hupp, *Chem. Soc. Rev.* **2009**, *38*, 1450.
[24] P. Horcajada, R. Gref, T. Baati, P. K. Allan, G. Maurin, P. Couvreur, G. Férey, R. E. Morris, C. Serre, *Chem. Rev.* **2012**, *112*, 1232.
[25] P. Falcaro, K. Okada, T. Hara, K. Ikigaki, Y. Tokudome, A. W. Thornton, A. J. Hill, T. Williams, C. Doonan, M. Takahashi, *Nat. Mater.* **2017**, *16*, 342.
[26] A. A. Talin, A. Centrone, A. C. Ford, M. E. Foster, V. Stavila, P. Haney, R. A. Kinney, V. Szalai, F. El Gabaly, H. P. Yoon, F. Léonard, M. D. Allendorf, *Science* **2014**, *343*, 66.
[27] S. Fujiwara, M. Hosoyamada, K. Tateishi, T. Uesaka, K. Ideta, N. Kimizuka, N. Yanai, *J. Am. Chem. Soc.* **2018**, *140*, 15606.
[28] T. Kitao, Y. Zhang, S. Kitagawa, B. Wang, T. Uemura, *Chem. Soc. Rev.* **2017**, *46*, 3108.
[29] S. Fujiwara, N. Matsumoto, K. Nishimura, N. Kimizuka, K. Tateishi, T. Uesaka, N. Yanai, *Angew. Chem. Int. Ed.* **2022**, *61*, e202115792.
[30] S. R. V. Parambil, F. A. Rahimi, R. Ghosh, S. Nath, T. K. Maji, *Inorg. Chem.* **2023**, *62*, 19312.
[31] T. Miura, T. Kitao, T. Uemura, *J. Phys. Chem. C* **2022**, *126*, 6628.
[32] V. Ţucureanu, A. Matei, A. M. Avram, *Crit. Rev. Anal. Chem.* **2016**, *46*, 502.
[33] T. Sasaki, Y. Yamada, S. Sato, *Anal. Chem.* **2018**, *90*, 10724.
[34] S. S. Zade, N. Zamoshchik, A. R. Reddy, G. Fridman-Marueli, D. Sheberla, M. Bendikov, *J. Am. Chem. Soc.* **2011**, *133*, 10803.
[35] R. Einholz, T. Fang, R. Berger, P. Grüninger, A. Früh, T. Chassé, R. F. Fink, H. F. Bettinger, *J. Am. Chem. Soc.* **2017**, *139*, 4435.
[36] I. Senkovska, F. Hoffmann, M. Fröba, J. Getzschmann, W. Böhlmann, S. Kaskel, *Microporous Mesoporous Mater.* **2009**, *122*, 93.
[37] H. Hayashi, N. Hieda, M. Yamauchi, Y. S. Chan, N. Aratani, S. Masuo, H. Yamada, *Chem. Eur. J.* **2020**, *26*, 15079.
[38] H. Takezawa, K. Shitozawa, M. Fujita, *Nat. Chem.* **2020**, *12*, 574.
[39] H. F. Bettinger, R. Mondal, M. Krasowska, D. C. Neckers, *J. Org. Chem.* **2013**, *78*, 1851.
[40] A. Jančařík, J. Holec, Y. Nagata, M. Šámal, A. Gourdon, *Nat. Commun.* **2022**, *13*, 223.
[41] R. Mondal, C. Tönshoff, D. Khon, D. C. Neckers, H. F. Bettinger, *J. Am. Chem. Soc.* **2009**, *131*, 14281.
[42] T. Kitao, T. Miura, R. Nakayama, Y. Tsutsui, Y. S. Chan, H. Hayashi, H. Yamada, S. Seki, T. Hitosugi, T. Uemura, *Nat. Synth.* **2023**, *2*, 848.
[43] R. Mondal, B. K. Shah, D. C. Neckers, *J. Am. Chem. Soc.* **2006**, *128*, 9612.
[44] K. Hubenko, A. Kusber, M. Naumann, B. Büchner, M. Knupfer, *J. Chem. Phys.* **2024**, *160*, 144708.
[45] H. Qu, C. Chi, *Org. Lett.* **2010**, *12*, 3360.
[46] T. Miyazaki, M. Watanabe, T. Matsushima, C.-T. Chien, C. Adachi, S.-S. Sun, H. Furuta, T. J. Chow, *Chem. Eur. J.* **2021**, *27*, 10677.
[47] B. J. Birks, *Photophysics of Aromatic Molecules*. Wiley-Interscience, London **1970**.
[48] M. Bixon, J. Jortner, J. Cortes, H. Heitele, M. E. Michel-Beyerle, *J. Phys. Chem.* **1994**, *98*, 7289.
[49] N. Nijegorodov, V. Ramachandran, D. P. Winkoun, *Spectrochim. Acta A* **1997**, *53*, 1813.
[50] I. Kaur, N. N. Stein, R. P. Kopreski, G. P. Miller, *J. Am. Chem. Soc.* **2009**, *131*, 3424.
[51] Y. Yang, E. R. Davidson, W. Yang, *Proc. Natl. Acad. Sci. USA* **2016**, *113*, E5098.
[52] D.-e. Jiang, S. Dai, *J. Phys. Chem. A* **2008**, *112*, 332.
[53] B. Purushothaman, M. Bruzek, S. R. Parkin, A.-F. Miller, J. E. Anthony, *Angew. Chem. Int. Ed.* **2011**, *50*, 7013.
[54] N. Zeitter, N. Hippchen, P. Baur, T. V. Unterreiner, F. Rominger, J. Freudenberg, U. H. F. Bunz, *Org. Mater.* **2024**, *6*, 12.
[55] G. Trinquier, G. David, J.-P. Malrieu, *J. Phys. Chem. A* **2018**, *122*, 6926.
[56] Y. Kawashima, T. Hamachi, A. Yamauchi, K. Nishimura, Y. Nakashima, S. Fujiwara, N. Kimizuka, T. Ryu, T. Tamura, M. Saigo, K. Onda, S. Sato, Y. Kobori, K. Tateishi, T. Uesaka, G. Watanabe, K. Miyata, N. Yanai, *Nat. Commun.* **2023**, *14*, 1056.

Manuscript received: May 20, 2025
Revised manuscript received: June 13, 2025
Version of record online: June 22, 2025